JOURNAL OF AGRICULTURAL AND FOOD CHEMISTRY



# Involvement of Caspases and Apoptosis-Inducing Factor in Bufotalin-Induced Apoptosis of Hep 3B Cells

CHUN-LI SU,[†] TING-YU LIN,[‡] CHUN-NAN LIN,[§] AND SHEN-JEU WON*[,‡]

Department of Nursing, Chang Jung Christian University, No. 396, Sec. 1, Changrong Road, Gueiren, Tainan 711, Taiwan, Department of Microbiology and Immunology, Medical College, National Cheng Kung University, No. 1, Ta-Hsueh Road, Tainan 701, Taiwan, and School of Pharmacy, Kaohsiung Medical University, No. 100, Shih-Chuan first Road, Kaohsiung 807, Taiwan

Bufotalin is one of the bufadienolides isolated from Formosan Ch'an Su, which is made of the skin and parotid glands of toads. Ingestion of toad venom results in severe morbidity and high mortality. Although Ch'an Su is clinically toxic, it has been used as an important traditional Chinese medicine for heart failure and pains. In this study, bufotalin-induced apoptosis in human hepatocellular carcinoma Hep 3B cells was investigated. The results indicate that externalization of phosphatidylserine, accumulation of sub-$G_1$ cells, fragmentation of DNA, and formation of apoptotic bodies were observed in bufotalin-treated Hep 3B cells. The signaling pathway might be via the activation of caspase-8, increase in mitochondrial tBid, disruption of mitochondrial membrane potential, and translocation of apoptosis-inducing factor (AIF). Active caspase-8 might activate caspase-9 and caspase-3 leading to the cleavage of nuclear PARP. Presence of AIF and cleaved PARP in the nuclei might lead to DNA fragmentation. Caspase-8 inhibitor (Z-IETD) or wide-ranging caspase inhibitor (Z-VAD) significantly suppressed the bufotalin-induced apoptosis, while the anti-Fas neutralization antibody had no effect. These data suggest that bufotalin-induced apoptosis in Hep 3B cells might involve caspases and AIF.

**KEYWORDS: Bufotalin; Ch'an Su; apoptosis; mitochondria; caspases; apoptosis-inducing factor**

## INTRODUCTION

Toad venom, also called Ch'an Su or toad poison, is made of skin and the parotid glands of toads (*1*). Ingestion of toad venom results in severe morbidity and high mortality (*2*). Besides nausea, vomiting, and abdominal discomfort, the majority of patients with Ch'an Su experience digitalis toxicity-like cardiac effects such as hyperkalaemia, bradycardia, artrioventricular conduction block, ventricular fibrillation, and sudden death (*1*). The major bioactive compounds in Ch'an Su are bufadienolides (*3*). More than 40 bufadienolides have been identified including bufalin, bufotalin, gamabufotalin, cinobufotagin, and resibufogenin (*4*).

Although Ch'an Su is clinically toxic, it exhibits pharmacological effects and has been used as an important traditional Chinese medicine for heart failure and pains (*3*). Recently, Ch'an Su has been revealed to display antitumor activities, and the major active constituents are a class of C-24 bufadienolides with an α-pyrone ring at C-17 such as bufalin, cinobufagin, and resibufogenin (*3, 5*−*7*). However, their molecular mechanisms remain unknown. The present study was carried out to determine the antitumor mechanism of bufotalin. The results suggest that bufotalin induced apoptosis of human hepatocellular carcinoma (HCC) Hep 3B cells via both caspase-related and caspase-unrelated signaling pathways.

## MATERIALS AND METHODS

**Isolation of Bufotalin.** Bufotalin (>98.9% purity) was purified from Formosan Ch'an Su (*Bufo bufo asiaticus* STEINDACHNER and *Bufo bankorensis* BORBOUR) obtained from Heng Hsin Chem. & Pharm. Co., Ltd. (Taipei Hsien, Taiwan) (*8*). Formosan Ch'an Su was extracted with methanol. Following fractionation with chloroform, bufotalin was obtained by chromatography on a silica gel using ethylacetate as an eluting agent (*8*). The structure of bufotalin is shown in **Figure 1A**, and the molecular weight was determined to be 444 ($C_{26}H_{36}O_6$).

**Chemicals.** Most of the chemicals were purchased from Sigma Chemical Co. (St. Louis, MO) unless otherwise indicated. Dulbecco's modified Eagle medium (DMEM) and fetal bovine serum (FBS) were purchased from Hyclone (Logan, UT). Sodium dodecylsulphate (SDS), dimethylsulfoxide (DMSO), and RNase A were purchased from Merck (Darmstadt, Germany). General caspase inhibitor Z-VAD and caspase-8 inhibitor Z-IETD were purchased from Santa Cruz Biotech (Santa Cruz, CA). Other reagents were obtained from

* To whom correspondence should be addressed. Tel: + 886 6 2744435. Fax: + 886 6 2082705. E-mail: a725@mail.ncku.edu.tw.
[†] Chang Jung Christian University.
[‡] National Cheng Kung University.
[§] Kaohsiung Medical University.

10.1021/jf802769g CCC: $40.75 
Published on Web 12/04/2008

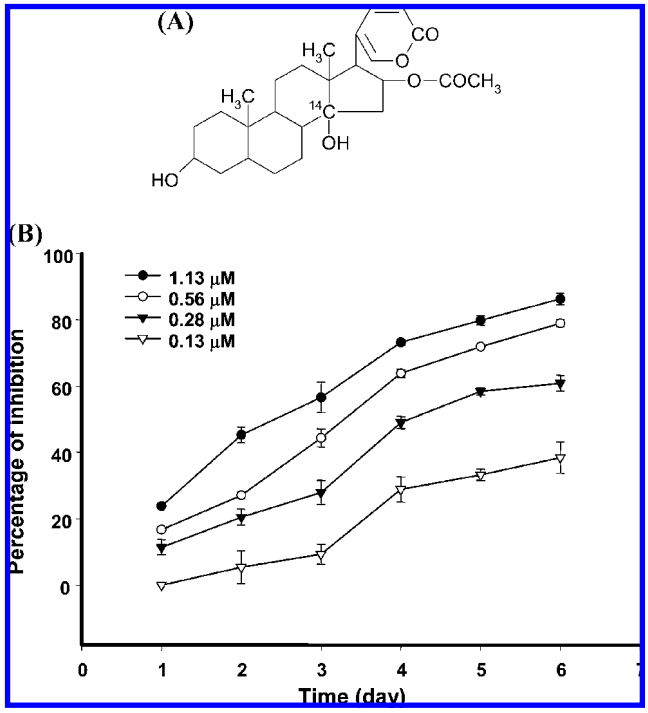


**Figure 1.** Cytoxicity of bufotalin. (**A**) Structure of bufotalin. (**B**) Growth inhibition of bufotalin on Hep 3B cells. Cells ($1.5 \times 10^3$) were cultured with complete DMEM containing various concentrations of bufotalin. At the indicated time points, viability of the cells was determined by MTT colorimetric assay. The experimental data was expressed as means ± SEM. Bufotalin was dissolved in DMSO. Before use, bufotalin was diluted with complete DMEM to yield the final desired experimental concentrations. Results were representative of three independent experiments.

the following sources: methanol (Wako, Osaka, Japan); proteinase K (BD Biosciences Clontech, Palo Alto, CA); and merocyanine 540 (MC 540, Calbiochem, La Jolla, CA). Goat polyclonal anti-Ku70, mouse monoclonal anti-Bcl-$X_L$ and antiapoptosis-inducing factor (AIF), and antimouse, antirabbit, and antigoat conjugated horseradish peroxidase (HRP) secondary antibodies were purchased from Santa Cruz Biotech (Santa Cruz, CA). Mouse monoclonal anticytochrome *c* and rabbit polyclonal antipoly(ADP-ribose) polymerase (PARP) antibodies were purchased from BD Pharmingen (San Diego, CA). Mouse monoclonal anticaspase-9 and anti-Fas (ZB-4) antibodies were purchased from Upstate Biotechnology (Lake Placid, NY). Other antibodies were purchased from the following sources: mouse monoclonal anticaspase-8 antibody (Cell Signaling Technology, Beverly, MA); mouse monoclonal anticaspase-3 and antisecond mitochondria-derived activator of caspase/direct IAP binding protein with low PI (Smac) antibodies (IMGENEX, San Diego, CA); rabbit polyclonal anti-Bid (Biosource, Camarillo, CA); antirabbit conjugated HRP secondary antibody (Amersham Pharmacia Biotech, Piscataway, NJ); anti-$\beta$-Actin antibody (Sigma, St. Louis, MO); and antimouse FITC-conjugated secondary antibody (Jackson ImmunoResearch Laboratories, Milan Analytica, La Roche, Switzerland).

**Cell Culture.** Human HCC Hep 3B cells, human colorectal carcinoma HT-29 cells, and human breast adenocarcinoma MCF7 cells were obtained from American type Culture Collection (ATCC, Rockville, MD). Cells were grown in complete DMEM in a humidified atmosphere with 5% $CO_2$ at 37 °C (9).

**Viability Assay.** Cell viability was determined by a modified colorimetric assay (9). Cells ($1.5 \times 10^3$) were cultured with complete DMEM for 1−6 days. At the indicated time points, 3-[4,5]-dimethylthiazol-2-yl)-2,5-diphenyltetra-zolium bromide (MTT) was added to each well to a final concentration of 0.5 mg/mL. After incubation, 10% SDS in 0.01 N HCl was added to each well and

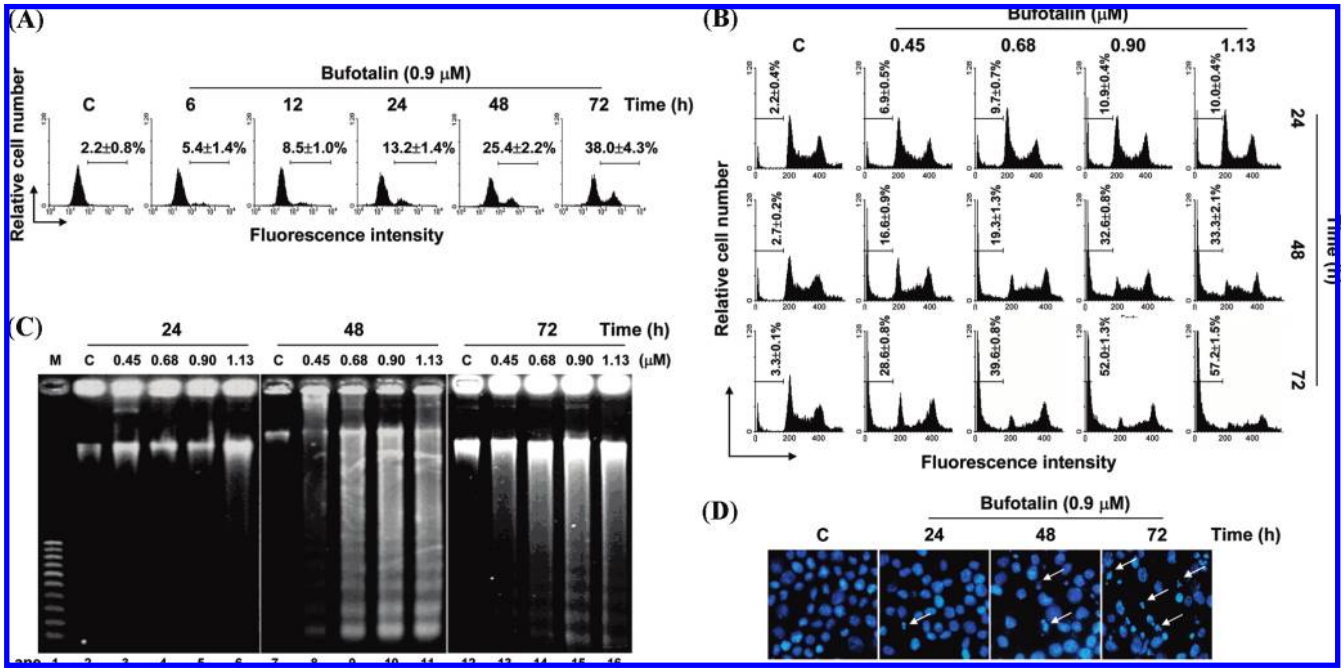


**Figure 2.** Induction of apoptosis. (**A**) Effect of bufotalin on translocation of phosphatidylserine. Cells ($2 \times 10^5$) incubated with 0.9 $\mu$M bufotalin for 6−72 h were stained with MC 540 and analyzed by flow cytometry. The percentage in the figure indicates the proportion of apoptotic cells with externalization of phosphatidylserine to the outer layer of the plasma membrane. (**B**) Effect of bufotalin on cell cycle distribution. Cells ($2 \times 10^5$) treated with the indicated conditions were stained with PI before flow cytometry. The percentage in the figure indicates the proportion of apoptotic cells arrested at the sub-$G_1$ phase. (**C**) Effect of bufotalin on DNA fragmentation. After treatment, the DNA fragments were separated on 1% agarose gels. M indicates the DNA molecular weight marker. (**D**) Effect of bufotalin on the formation of apoptotic bodies. Cells ($2 \times 10^6$) incubated with 0.9 $\mu$M bufotalin for 24−72 h were stained with Hoechst 33258 and analyzed by fluorescence microscopy. The arrowhead indicates the formation of apoptotic bodies. Control cells (C) were treated with 0.1% of DMSO. Results were representative of three independent experiments.

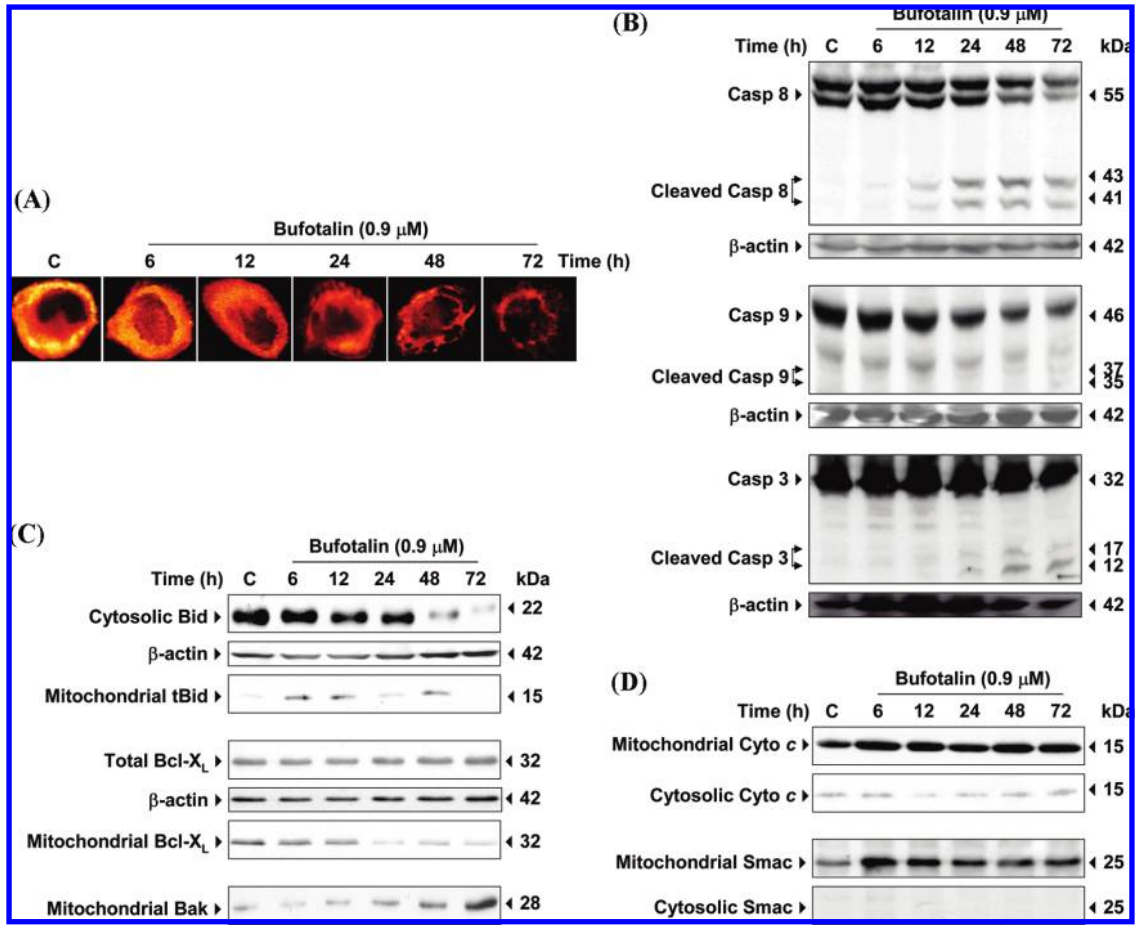


**Figure 3.** Effect of bufotalin on mitochondria and their related protein expressions. (**A**) Bufotalin induced change of $\Delta\psi_m$ in Hep 3B cells. Cells ($2 \times 10^5$) were incubated with 0.9 $\mu$M bufotalin for 6−72 h. After staining with rhodamine 123, the cells were examined by confocal microscopy. (**B**) Expression of caspase (Casp)-8, -9, and -3 in total cell lysates. (**C**) Distribution of Bid, tBid, Bcl-$X_L$, and Bak. (**D**) Distribution of cytochrome *c* (Cyto *c*) and Smac. Total, cytosolic, mitochondrial, or nuclear proteins were subjected to immunoblotting. $\beta$-Actin was used as the loading control. Results were representative of three independent experiments.

incubated overnight. The absorbance of each well was measured in a microplate reader at 590 nm on a Multiscan photometer (MRX II, Dynatech, McLean, VA).

**Flow Cytometric Analysis of Phosphatidylserine Translocation and Cell Cycle Distribution.** The analysis was assessed according to the previous report (*9*). To measure phosphatidylserine translocation, cells were resuspended in HEPES buffer solution (HBS) containing 20 $\mu$g/mL MC 540 and examined by a FACSan flow cytometer (Becton Dickson, Mountain View, CA) with an excitation wavelength of 488 nm and emission wavelength of 675 nm. For cell cycle analysis, cells were resuspended in HBS containing 40 $\mu$g/mL of propidium iodide (PI) and 100 mg/mL RNase A. After 30 min, The PI-stained cells were sorted by flow cytometry.

**DNA Fragmentation Assay.** As previously described (*9*), cells were lysed with lysis buffer containing 10 mM Tris-HCl (pH 7.6), 1% IGEPAL CA-630 (NP-40), and 20 mM EDTA at 37 °C for 20 min. After centrifugation, the supernatants were incubated with a solution containing 1% SDS and 4 mg/mL RNase A for 2 h, followed by incubation with 200 $\mu$g/mL proteinase K for 2 h. DNA was precipitated overnight. The DNA samples were separated on 1% agarose gel and examined by exposing to UV light after staining with ethidium bromide.

**Fluorescence Microscopic Determination of Apoptotic Bodies.** For evaluating the formation of apoptotic bodies (*10*), cells were fixed with 3.7% paraformaldehyde in PBS for 5 min and stained with 0.5 $\mu$g/mL Hoechst 33258 in PBS at 37 °C for 30 min before microscopy (Leica DMRBE microscope).

**Determination of Mitochondrial Membrane Potential ($\Delta\psi$m) and AIF Translocation by Confocal Microscopy.** As previously described (*9*), cells on coverslips were stained with 5 $\mu$M rhodamine 123 and 0.5 $\mu$g/mL Hoechst 33258. After fixing with cold methanol (−20 °) for 5 min and permeabilizing with cold acetone (−20 °) for 5 min, the cells were rinsed with PBS containing sodium azide (15 mM). After blocking with PBS containing 5% (w/v) bovine serum albumin (BSA) and 0.1 M methylamine for 1 h, the cells were incubated with anti-AIF antibody overnight and then with FITC-conjugated secondary antibody in 5% (w/v) BSA for 3 h at room temperature. The cells were then mounted with mounting media containing 50% (v/v) glycerol in PBS containing 2% (w/v) *p*-phenylenediamine and examined immediately by a Leica TCSNT laser scanning confocal imaging system coupled to a Leica DMRBE microscope.

**Immunoblotting.** As described previously (*9*), total cell lysates were obtained by incubating cells with lysis buffer containing 10 mM Tris-HCl (pH 7.9), 5 mM EDTA, 0.15 M NaCl, 5 mM $Na_2HPO_4 \cdot 12\ H_2O$, 5 mM $NaH_2PO_4 \cdot 2\ H_2O$, 5 mM $Na_4P_2O_7 \cdot 10\ H_2O$, 1% (w/v) Triton X-100, 10 mM NaF, 10 mM $NaN_3$, and 1 tablet of complete protease inhibitor cocktail (Boehringer, Mannheim, Germany). After centrifugation at 15,000*g* for 10 min to remove the unbroken cells, the supernatants were subjected to immunoblotting (*10*). For nuclear proteins preparation (*9*), cells were incubated with buffer A containing 10 mM HEPES (pH 7.9), 10 mM NaF, 0.5 mM dithiothreitol (DTT), 5 mM $MgC1_2$, 3 mM $Na_3VO_4$, 10 mM KC1, 0.5 mM penylmethylsulfonyl fluoride (PMSF), 2 $\mu$g/mL leupeptin, and 2 $\mu$g/mL pepstatin A on ice for 20 min. After centrifugation at 11,000*g* for 20 s, the pellets were dissolved in buffer B containing 20 mM HEPES (pH 7.9), 420 mM NaCl, 0.2 mM EDTA, 25% glycerol, 1.5 mM $MgC1_2$, 3 mM $Na_3VO_4$, 10 mM NaF, 0.5 mM DTT, 0.5 mM PMSF, 2 $\mu$g/mL leupeptin, and 2 $\mu$g/mL pepstatin A for immunoblotting. To obtain cytosolic and mitochondrial fractions (*9*), cells were incubated with TSE buffer containing 0.25 M sucrose,

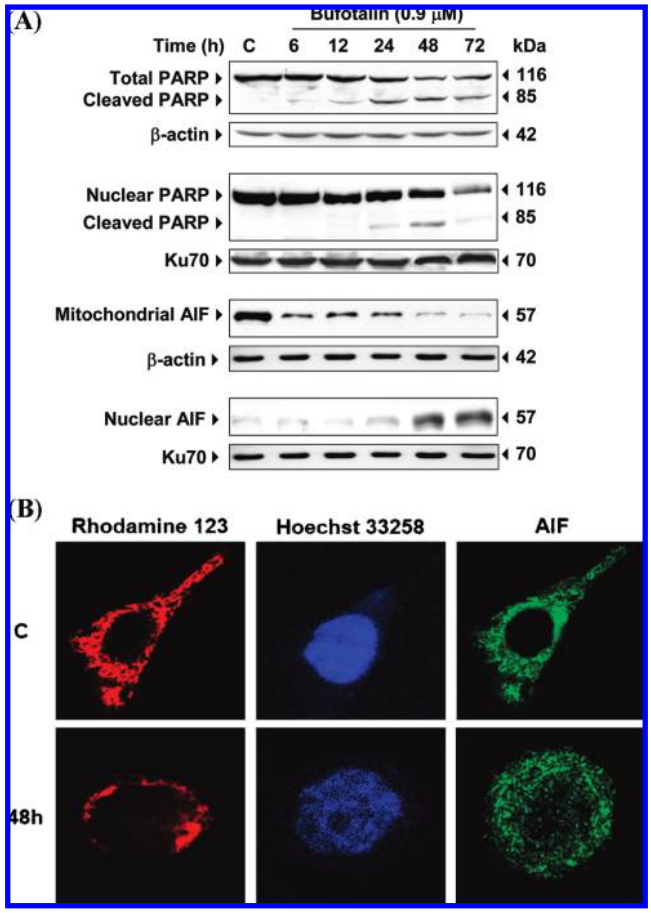


**Figure 4.** Expression of proteins related to DNA fragmentation. (**A**) Expression of PARP and AIF by Immunoblotting. Cells ($2 \times 10^5$) were incubated with 0.9 $\mu$M bufotalin for 6−72 h. Ku70 and $\beta$-Actin were used as the loading control. (**B**) Immunofluorescense analysis of AIF. Cells ($2 \times 10^6$) were incubated with 0.9 $\mu$M bufotalin for 48 h. Rhodamine 123, Hoechst 33258, and anti-AIF antibody were used to stain mitochondria, nuclei, and AIF, respectively. The cells were then analyzed by confocal microscopy. Results were representative of three independent experiments.

10 mM Tris, and 0.1 mM EDTA (pH 7.4), followed by braking with 10 strokes of a Teflon pestle in a Dounce homogenizer (Glas-Col, Terre Haute, IN). After centrifugation at 750*g* at 4 °C for 30 min, the supernatants were centrifuged at 12,000*g* for 30 min at 4 °C. The supernatants were centrifuged again at 100,000*g* for 1 h. The supernatants were used as the cytosolic fractions for immunoblotting. The pellets dissolved in lysis buffer were used as the mitochondrial fractions for immunoblotting.

## RESULTS

**Cytotoxic Effect of Bufotalin on Human Cancer Cells.** Viability of bufotalin-treated Hep 3B, HT-29, and MCF7 cells were determined by colorimetric assay. The 50% inhibitory concentrations ($IC_{50}$) of bufotalin at day 6 were 0.24 ± 0.02, 0.23 ± 0.03, and 0.15 ± 0.02 $\mu$M, respectively. The clonogenic inhibition of bufotalin on these cells was also evaluated by a two-layer soft agar system. The $IC_{50}$ values of bufotalin for these cells to form colonies were calculated to be 0.12 ± 0.05, 0.09 ± 0.03, and 0.15 ± 0.02 $\mu$M, respectively. In order to understand the antitumor effect of bufotalin on HCC, Hep 3B cells were used for further study. Daily evaluation revealed that bufotalin significantly decreased the viability of Hep 3B cells when the incubation time and bufotalin dosage increased (**Figure 1B**). Up to 80% of growth inhibition was observed when Hep 3B cells were treated with 1.13 $\mu$M bufotalin for 6 consecutive days. Bufotalin also suppressed Hep 3B cells to form colonies on soft agar in a dose-related manner. The formation of colonies was almost completely inhibited by 0.23 $\mu$M bufotalin at day 14 post-treatment (data not shown).

**Induction of Apoptosis in Hep 3B Cells by Bufotalin.** To test whether bufotalin cytotoxicity in Hep 3B cells was caused by apoptosis, the MC 540 binding assay (*11*) was performed. **Figure 2A** shows that the percentage of cells with MC 540 staining on the outer layer of plasma membrane was increased, ranging from 5.4% at 6 h to 38% at 72 h after treatment of 0.9 $\mu$M bufotalin. To further confirm the process of apoptosis, cells were stained with PI for cell cycle analysis. As shown in **Figure 2B**, bufotalin (1.13 $\mu$M) significantly elevated the percentage of Hep 3B cells at the sub-$G_1$ phase in a time-related manner, ranging from 10.0% at 24 h to 57.2% at 72 h. Dose-related increase in the population of sub-$G_1$ cells was also displayed from 2.7 and 3.3% in nontreated to 33.3 and 57.2% in those treated with 1.13 $\mu$M bufotalin for 48 and 72 h, respectively. Agarose gel electrophoresis also exhibited fragments of DNA when cells were treated with more than 0.45 $\mu$M of bufotalin for more than 48 h (**Figure 2C**). Morphological analysis of bufotalin-treated Hep 3B cells was conducted after staining cells with Hoechst 33258 to examine the formation of apoptotic bodies. As shown in **Figure 2D**, apoptotic bodies with condensed chromatin and degraded nuclei were gradually increased as incubation time increased from 24 to 72 h.

**Effect of Bufotalin on Mitochondria-Related Signaling Pathways.** In order to determine if mitochondria were involved in bufotalin-induced apoptosis, changes of $\Delta\psi$m in bufotalin-treated Hep 3B cells were determined by confocal microscopy. As shown in **Figure 3A**, bufotalin gradually and significantly reduced the brightness of rhodamine 123 staining when incubation time increased from 6 to 72 h. Caspase-8, a key initiator caspase, may act upstream of mitochondria (*12*). In **Figure 3B**, expression of full length (inactive) caspase-8 was significantly reduced after 48 h of incubation, while expression of cleaved (active) caspase-8 first appeared at 6 h and reached the peak level at 24−72 h after treatment of 0.9 $\mu$M bufotalin. Caspase-9 is another important protein in apoptotic cascades. In **Figure 3B**, the intensity of full length caspase-9 was decreased, whereas that of cleaved caspase-9 was increased slightly at 12 h. As expected, downstream effecter caspase-3 was also cleaved into its active form, which was first observed at 6 h and peaked at 48−72 h of treatment.

Mitochondrial homeostasis could also be influenced directly by proteins of the Bcl-2 family (*13*). The change of $\Delta\psi$m (**Figure 3A**) and activation of caspase-8 (**Figure 3B**) implied the involvement of Bid in bufotalin-induced apoptosis (*13*). As shown in **Figure 3C**, bufotalin significantly decreased cytosolic Bid and increased mitochondrial tBid. The increase in the level of mitochondrial tBid was first detected at 6 h and sustained to 48 h of treatment. Bcl-$X_L$ is an antiapoptotic protein, which prevents mitochondrial dysfunction by interacting with Bax (*14*). In **Figure 3C**, expression of mitochondrial Bcl-$X_L$ was slightly suppressed at 6−12 h, and significant reduction in mitochondrial Bcl-$X_L$ was observed at 24−72 h. However, total expression of Bcl-$X_L$ remained the same. Bak is a pro-apoptotic protein, which can oligomerize with tBid and results in the dysfunction of mitochondria (*15*). In this study, increase in mitochondrial

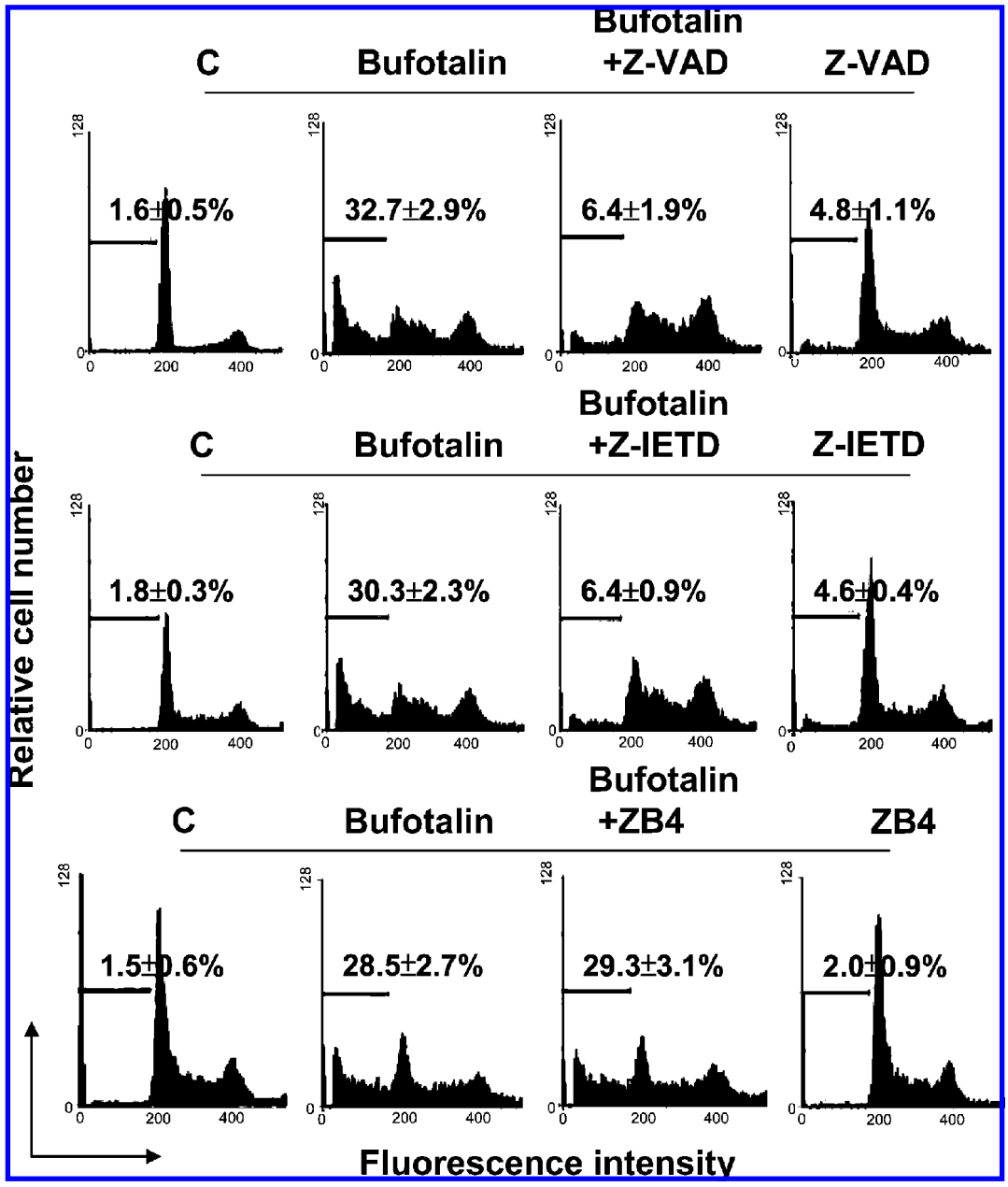


**Figure 5.** Effect of general caspase inhibitor (Z-VAD), caspase-8 inhibitor (Z-IETD), or anti-Fas antibody (ZB-4) on the apoptosis of Hep 3B cells. Cells ($2 \times 10^6$) were pretreated with 15 $\mu$M Z-VAD or Z-IETD, or with 100 ng/mL ZB-4 for 1 h prior to the addition of 0.9 $\mu$M bufotalin for 48 h. The cells were harvested and stained with PI for flow cytometry. The percentage in the figure indicates the proportion of apoptotic cells arrested at the sub-$G_1$ phase. Results were representative of three independent experiments.

expression of Bak was also observed in response to bufotalin (**Figure 3C**). Recent reports also indicate that changes of $\Delta\psi$m can cause the release of mitochondrial proteins such as cytochrome *c* and Smac into cytosol to promote apoptosis (*16*, *17*). Interestingly enough, neither cytochrome *c* nor Smac expression was decreased in the mitochondria or elevated in the cytosol with treatment of bufotalin (**Figure 3D**).

**Molecules Involved in Bufotalin-Induced DNA Fragmentation.** To elucidate possible reasons for bufotalin-induced fragmentation of DNA (**Figure 2C**), expressions of related proteins were determined by immunoblotting. As expected, expression of full-length PARP, a substrate of caspase-3 (*18*, *19*), was suppressed and that of cleaved PARP was elevated in whole cell lysate (**Figure 4A**). More specifically, nuclear full-length PARP was decreased in a time-related manner, and the cleaved form of PARP in the nuclei was significantly increased at 24 h of treatment (**Figure 4A**). AIF is another possible protein that participates in the degradation of DNA (*20*). As indicated in **Figure 4A**, mitochondrial AIF was decreased in a time-related manner, and nuclear AIF was elevated at 24 h and peaked at 48−72 h of bufotalin treatment. The movement of AIF from the mitochondria to the nuclei was further confirmed by confocal microscopy. As shown in **Figure 4B**, the fluorescence pattern of AIF in the control cells was similar to that of the mitochondria stained with rhodamine 123, whereas treatment of bufotalin changed the fluorescence pattern of AIF to that of the nuclei stained with Hoechst 33258.

**Role of Caspases and Fas in Bufotalin-Induced Apoptosis.** To further determine whether bufotalin-induced cell death is caspase-dependent, wide-ranging caspase inhibitor Z-VAD was used. In **Figure 5**, bufotalin (0.9 $\mu$M) alone caused 32.7% of cells to undergo apoptosis at 48 h, whereas the addition

of Z-VAD (15 $\mu$M) reduced the apoptosis rate to 6.4%. Similar results were obtained by using caspase-8 specific inhibitor Z-IETD (15 $\mu$M) for 48 h. To determine if Fas was involved (*21*) in bufotalin-induced apoptosis, anti-Fas neutralization antibody ZB-4 (100 ng/mL) was used. Interestingly enough, ZB-4 did not alter the proportion of apoptotic cells in the presence of bufotalin (**Figure 5**).

## DISCUSSION

In this study, all tested carcinoma cells are sensitive to the treatment of bufotalin with low $IC_{50}$ values. In HCC Hep 3B cells, the cytotoxicity of bufotalin is due to the induction of apoptosis (**Figure 2A−D**). This apoptotic signaling cascade seems to begin at the activation of caspase-8 (**Figure 3B**) without interacting with the Fas receptor (**Figure 5**), although the expression of Fas protein was detected in the Hep 3B cells (data not shown). Similar results have been observed, in which caspase-8 was activated in a Fas-independent induction of apoptosis by therapeutic drugs (*22*). Expression of Fas protein in HCC has also been reported to be lower than that in noncancerous liver cells (*23*). Activation of caspase-8 might be via the suppression of cellular-FLICE inhibitory protein (c-FLIP, an endogenous caspase-8 inhibitor) (*24, 25*) or the degradation of the cellular inhibitor of apoptosis protein (cIAP1 and cIAP2) (*26*). Caspase-8 is an upstream regulator of mitochondria by cleaving Bid into tBid to induce changes in $\Delta\psi$m (*27*). In this study, we have observed the activation of caspase-8 (**Figure 3B**), the translocation of tBid from the cytosol to the mitochondria (**Figure 3C**), and the disruption of $\Delta\psi$m (**Figure 3A**) at 6 h of treatment. Besides Bid, Bak is another member of the Bcl-2 family proteins (*28*). In response to specific stimuli, tBid migrates to the mitochondria, binds to its mitochondrial partner Bak, and results in allosteric conformational activation of Bak (*29*). In this study, as incubation time increased, slight elevation in mitochondrial Bak was exhibited (**Figure 3C**). Bcl-$X_L$ is another member of the Bcl-2 family, which can bind to BH3 domain-only molecules such as Bid and attenuate Bak-mediated mitochondrial apoptosis (*14*). In **Figure 3C**, Bcl-$X_L$ in the mitochondrial fraction was apparently inhibited at 6 h of treatment. This suppression in mitochondrial Bcl-$X_L$ might therefore enhance the process of apoptosis. Ku70, a subunit of the protein complex essential for nonhomologous DNA double-strand break repair, can also inhibit the apoptotic action of Bax by inhibiting its translocation from the cytosol to mitochondria (*30, 31*). However, in this study, the expression of cytosolic Ku70 was not changed throughout the experimental periods (data not shown). The data presented here suggest that changes of $\Delta\psi$m in bufotalin-treated Hep 3B cells might be due to caspase-8-induced increase in tBid as well as suppression in Bcl-$X_L$ expression on mitochondria.

Direct activation of caspase-9 by caspase-8 has been reported (*32*). Activation of caspase-9 can occur as well by forming a complex of caspase-9, Apaf-1, and cytochrome *c* (*33*). Since translocation of cytochrome *c* to the cytosol was not observed in response to bufotalin (**Figure 3D**), activation of caspase-9 might be occurring directly by active caspase-8 rather than by forming the complex. In addition, active caspase-8 or -9 alone can directly cleave and activate caspase-3 for apoptosis (*12*). **Figure 3B** indicates that active forms of caspase-8 and -3 first appeared at 6 h, whereas that of caspase-9 was not observed until a later time point (>12 h). These data imply that activation of caspase-3 at the early time point (6 h) might be due in part to the activation of caspase-8 (*34*). In this study, we also observed the suppression of X-linked apoptosis-inhibiting protein (XIAP) in response to bufotalin (data not shown). XIAP has been reported to interact directly with caspase-3, Smac, or cytochrome *c*, leading to an attenuation of the process of apoptosis (*35−37*). Since we did not detect the translocation of either Smac or cytochrome *c* to the cytosol (**Figure 3D**), XIAP may mainly interact with caspase-3 in the cells. This decrease in XIAP expression may further ensure the activity of caspase-3.

During apoptosis, PARP has been reported to be proteolyzed directly by active caspase-3 and results in the inactivation of PARP for DNA repair, and therefore leads to the fragmentation of DNA (*18, 19*). Active caspase-3 also catalyzes DNA fragmentation factor (DFF)-45 and DFF-35, both of which can bind to DFF-40 and prevent it from translocating to the nuclei for nucleosomal DNA degradation (*38, 39*). In the present study, DFF-40 failed to be detected in the nuclei in response to bufotalin (data not shown). Upon apoptosis stimuli, AIF can also be liberated from mitochondria to nuclei to trigger DNA fragmentation (*20*). Here, we have demonstrated the translocation of AIF by immunoblotting and confocal microscopy (**Figure 4A** and **B**). Therefore, bufotalin induced DNA fragmentation (**Figure 2C**) might be due to the nuclear expression of cleaved PARP and AIF.

Translocation of AIF from mitochondria to nuclei has been reported to induce apoptosis in a caspase-independent manner (*20*). In conjunction with the activation of caspases (**Figure 3B**) and significant decrease in bufotalin-induced apoptosis by adding either caspase-8 specific inhibitor or wide-ranging caspase inhibitor (**Figure 5**), bufotalin-induced apoptosis might proceed via both caspase-related and caspase-unrelated pathways.

In conclusion, the cytotoxicity of bufotalin on HCC Hep 3B cells was due to the induction of apoptosis. Activation of caspases and release of AIF resulted in the fragmentation of DNA.

## ABBREVIATION USED

AIF, apoptosis-inducing factor; DFF, DNA fragmentation factor; HCC, human hepatocellular carcinoma; MTT, 3-(4,5-dimethylthiazol-2-yl)-2,5-diphenyltetrazolium bromide; PARP, poly(ADP-ribose) polymerase; PI, propidium iodide; Smac, second mitochondria-derived activator of caspase/direct IAP binding protein with low pI; XIAP, X-linked apoptosis-inhibiting protein; $\Delta\psi_m$, mitochondrial membrane potential.

## LITERATURE CITED

(1) Gowda, R. M.; Cohen, R. A.; Khan, I. A. Toad venom poisoning: resemblance to digoxin toxicity and therapeutic implications. *Heart* **2003**, *89*, e14.

(2) Jan, S. L.; Chen, F. L.; Hung, D. Z.; Chi, C. S. Intoxication after ingestion of toad soup: report of two cases. *Zhonghua Min Guo Xiao Er Ke Yi Xue Hui Za Zhi* **1997**, *38*, 477–480.

(3) Ye, M.; Guo, H.; Guo, H.; Han, J.; Guo, D. Simultaneous determination of cytotoxic bufadienolides in the Chinese medicine ChanSu by high-performance liquid chromatography coupled with photodiode array and mass spectrometry detections. *J. Chromatogr., B* **2006**, *838*, 86–95.

(4) Ye, M.; Guo, D. A. Analysis of bufadienolides in the Chinese drug ChanSu by high-performance liquid chromatography with atmospheric pressure chemical ionization tandem mass spectrometry. *Rapid Commun. Mass Spectrom.* **2005**, *19*, 1881–1892.

(5) Jing, Y.; Ohizumi, H.; Kawazoe, N.; Hashimoto, S.; Masuda, Y.; Nakajo, S.; Yoshida, T.; Kuroiwa, Y.; Nakaya, K. Selective inhibitory effect of bufalin on growth of human tumor cells *in vitro*: association with the induction of apoptosis in leukemia HL-60 cells. *Jpn. J. Cancer Res.* **1994**, *85*, 645–651.
(6) Watabe, M.; Masuda, Y.; Nakajo, S.; Yoshida, T.; Kuroiwa, Y.; Nakaya, K. The cooperative interaction of two different signaling pathways in response to bufalin induces apoptosis in human leukemia U937 cells. *J. Biol. Chem.* **1996**, *271*, 14067–14072.
(7) Watabe, M.; Kawazoe, N.; Masuda, Y.; Nakajo, S.; Nakaya, K. Bcl-2 protein inhibits bufalin-induced apoptosis through inhibition of mitogen-activated protein kinase activation in human leukemia U937 cells. *Cancer Res.* **1997**, *57*, 3097–3100.
(8) Lin, C. N.; Chung, M. I.; Wang, E. C.; Chen, I. J.; Cheng, S. C.; Arisawa, M.; Shimizu, M.; Morita, N. Studies on the components of Formasan Ch'an Su (I): Isolation of a new indole base, dehydrobufotonin. *Shoyakugaku Zasshi* **1984**, *38*, 175–177.
(9) Lee, J. C.; Lee, C. H.; Su, C. L.; Huang, C. W.; Liu, H. S.; Lin, C. N.; Won, S. J. Justicidin A decreases the level of cytosolic Ku70 leading to apoptosis in human colorectal cancer cells. *Carcinogenesis* **2005**, *26*, 1716–1730.
(10) Su, C. L.; Wu, C. J.; Chen, F. N.; Wang, B. J.; Sheu, S. R.; Won, S. J. Supernatant of bacterial fermented soybean induces apoptosis of human hepatocellular carcinoma Hep 3B cells via activation of caspase 8 and mitochondria. *Food Chem. Toxicol.* **2007**, *45*, 303–314.
(11) Chang, M. Y.; Won, S. J.; Yang, B. C.; Jan, M. S.; Liu, H. S. Selective activation of Ha-ras(val12) oncogene increases susceptibilityof NIH/3T3 cells to TNF-alpha. *Exp. Cell Res.* **1999**, *248*, 589–598.
(12) Roth, W.; Reed, J. C. Apoptosis and cancer: when BAX is TRAILing away. *Nat. Med.* **2002**, *8*, 216–218.
(13) Hengartner, M. O. The biochemistry of apoptosis. *Nature* **2000**, *407*, 770–776.
(14) Cheng, E. H.; Wei, M. C.; Weiler, S.; Flavell, R. A.; Mak, T. W.; Lindsten, T.; Korsmeyer, S. J. BCL-2, BCL-$X_L$ sequester BH3 domain-only molecules preventing BAX- and BAK-mediated mitochondrial apoptosis. *Mol. Cell* **2001**, *8*, 705–711.
(15) Korsmeyer, S. J.; Wei, M. C.; Saito, M.; Weiler, S.; Oh, K. J.; Schlesinger, P. H. Pro-apoptotic cascade activates BID, which oligomerizes BAK or BAX into pores that result in the release of cytochrome *c*. *Cell Death Differ.* **2000**, *7*, 1166–1173.
(16) Jemmerson, R.; LaPlante, B.; Treeful, A. Release of intact, monomeric cytochrome *c* from apoptotic and necrotic cells. *Cell Death Differ.* **2002**, *9*, 538–548.
(17) Zhang, X. D.; Zhang, X. Y.; Gray, C. P.; Nguyen, T.; Hersey, P. Tumor necrosis factor-related apoptosis-inducing ligand-induced apoptosis of human melanoma is regulated by Smac/DIABLO release from mitochondria. *Cancer Res.* **2001**, *61*, 7339–7348.
(18) Martin, S. J.; Green, D. R. Protease activation during apoptosis: death by a thousand cuts. *Cell* **1995**, *82*, 349–352.
(19) Soldani, C.; Lazze, M. C.; Bottone, M. G.; Tognon, G.; Biggiogera, M.; Pellicciari, C. E.; Scovassi, A. I. Poly(ADP-ribose) polymerase cleavage during apoptosis: When and where. *Exp. Cell Res.* **2001**, *269*, 193–201.
(20) Susin, S. A.; Lorenzo, H. K.; Zamzami, N.; Marzo, I.; Snow, B. E.; Brothers, G. M.; Mangion, J.; Jacotot, E.; Costantini, P.; Loeffler, M.; Larochette, N.; Goodlett, D. R.; Aebersold, R.; Siderovski, D. P.; Penninger, J. M.; Kroemer, G. Molecular characterization of mitochondrial apoptosis-inducing factor. *Nature* **1999**, *397*, 441–446.
(21) Natoli, G.; Ianni, A.; Costanzo, A.; De Petrillo, G.; Ilari, I.; Chirillo, P.; Balsano, C.; Levrero, M. Resistance to Fas-mediated apoptosis in human hepatoma cells. *Oncogene* **1995**, *11*, 1157–1164.
(22) You, K. R.; Shin, M. N.; Park, R. K.; Lee, S. O.; Kim, D. G. Activation of caspase-8 during N-(4-hydroxyphenyl)retinamide-induced apoptosis in Fas-defective hepatoma cells. *Hepatology* **2001**, *34*, 1119–1127.
(23) Higaki, K.; Yano, H.; Kojiro, M. Fas antigen expression and its relationship with apoptosis in human hepatocellular carcinoma and noncancerous tissues. *Am. J. Pathol.* **1996**, *149*, 429–437.
(24) Roy, A.; Hong, J. H.; Lee, J. H.; Lee, Y. T.; Lee, B. J.; Kim, K. S. *In vitro* activation of procaspase-8 by forming the cytoplasmic component of the death-inducing signaling complex (cDISC). *Mol. Cells* **2008**, *26*, 165–170.
(25) Ganten, T. M.; Haas, T. L.; Sykora, J.; Stahl, H.; Sprick, M. R.; Fas, S. C.; Krueger, A.; Weigand, M. A.; Grosse-Wilde, A.; Stremmel, W.; Krammer, P. H.; Walczak, H. Enhanced caspase-8 recruitment to and activation at the DISC is critical for sensitisation of human hepatocellular carcinoma cells to TRAIL-induced apoptosis by chemotherapeutic drugs. *Cell Death Differ.* **2004**, *11* (Suppl 1), S86−96.
(26) Wang, L.; Du, F.; Wang, X. TNF-alpha induces two distinct caspase-8 activation pathways. *Cell* **2008**, *133*, 693–703.
(27) Li, H.; Zhu, H.; Xu, C. J.; Yuan, J. Cleavage of BID by caspase 8 mediates the mitochondrial damage in the Fas pathway of apoptosis. *Cell* **1998**, *94*, 491–501.
(28) Adams, J. M.; Cory, S. The Bcl-2 protein family: arbiters of cell survival. *Science* **1998**, *281*, 1322–1326.
(29) Wei, M. C.; Lindsten, T.; Mootha, V. K.; Weiler, S.; Gross, A.; Ashiya, M.; Thompson, C. B.; Korsmeyer, S. J. tBID, a membrane-targeted death ligand, oligomerizes BAK to release cytochrome *c*. *Genes Dev.* **2000**, *14*, 2060–2071.
(30) Walker, J. R.; Corpina, R. A.; Goldberg, J. Structure of the Ku heterodimer bound to DNA and its implications for double-strand break repair. *Nature* **2001**, *412*, 607–614.
(31) Mancinelli, F.; Caraglia, M.; Budillon, A.; Abbruzzese, A.; Bismuto, E. Molecular dynamics simulation and automated docking of the pro-apoptotic Bax protein and its complex with a peptide designed from the Bax-binding domain of anti-apoptotic Ku70. *J. Cell. Biochem.* **2006**, *99*, 305–318.
(32) McDonnell, M. A.; Wang, D.; Khan, S. M.; Vander Heiden, M. G.; Kelekar, A. Caspase-9 is activated in a cytochrome *c*-independent manner early during TNFalpha-induced apoptosis in murine cells. *Cell Death Differ.* **2003**, *10*, 1005–1015.
(33) Li, P.; Nijhawan, D.; Budihardjo, I.; Srinivasula, S. M.; Ahmad, M.; Alnemri, E. S.; Wang, X. Cytochrome *c* and dATP-dependent formation of Apaf-1/caspase-9 complex initiates an apoptotic protease cascade. *Cell* **1997**, *91*, 479–489.
(34) Scaffidi, C.; Fulda, S.; Srinivasan, A.; Friesen, C.; Li, F.; Tomaselli, K. J.; Debatin, K. M.; Krammer, P. H.; Peter, M. E. Two CD95 (APO-1/Fas) signaling pathways. *EMBO J.* **1998**, *17*, 1675–1687.
(35) Deveraux, Q. L.; Takahashi, R.; Salvesen, G. S.; Reed, J. C. X-linked IAP is a direct inhibitor of cell-death proteases. *Nature* **1997**, *388*, 300–304.
(36) Wu, G.; Chai, J.; Suber, T. L.; Wu, J. W.; Du, C.; Wang, X.; Shi, Y. Structural basis of IAP recognition by Smac/DIABLO. *Nature* **2000**, *408*, 1008–1012.
(37) Deveraux, Q. L.; Roy, N.; Stennicke, H. R.; Van Arsdale, T.; Zhou, Q.; Srinivasula, S. M.; Alnemri, E. S.; Salvesen, G. S.; Reed, J. C. IAPs block apoptotic events induced by caspase-8 and cytochrome *c* by direct inhibition of distinct caspases. *EMBO J.* **1998**, *17*, 2215–2223.
(38) Enari, M.; Sakahira, H.; Yokoyama, H.; Okawa, K.; Iwamatsu, A.; Nagata, S. A caspase-activated DNase that degrades DNA during apoptosis, and its inhibitor ICAD. *Nature* **1998**, *391*, 43–50.
(39) Jayanthi, S.; Deng, X.; Noailles, P. A.; Ladenheim, B.; Cadet, J. L. Methamphetamine induces neuronal apoptosis via cross-talks between endoplasmic reticulum and mitochondria-dependent death cascades. *FASEB J.* **2004**, *18*, 238–251.

**Received for review September 8, 2008. Revised manuscript received November 11, 2008. Accepted November 13, 2008. This study was supported by grants from the National Science Council, Taiwan, Republic of China (NSC 95-2313-B-309-001; NSC 96-2313-B-309-001-MY2).**

JF802769G